

Elastic properties of proteins: insight on the folding process and evolutionary selection of native structures

Cristian Micheletti¹, Gianluca Lattanzi² and Amos Maritan^{1,3}

(1) *International School for Advanced Studies (S.I.S.S.A.) and INFM, Via Beirut 2-4, 34014 Trieste, Italy*

(2) *Hahn-Meitner Institut, Abt. SF5, Glienicker Str. 100, 14109 Berlin, Germany and*

(3) *The Abdus Salam International Center for Theoretical Physics, Trieste, Italy.*

(Dated: February 20, 2019)

We carry out a theoretical study of the vibrational and relaxation properties of naturally-occurring proteins with the purpose of characterizing both the folding and equilibrium thermodynamics. By means of a suitable model we provide a full characterization of the spectrum and eigenmodes of vibration at various temperatures by merely exploiting the knowledge of the protein native structure. It is shown that the rate at which perturbations decay at the folding transition correlates well with experimental folding rates. This validation is carried out on a list of about 30 two-state folders. Furthermore, the qualitative analysis of residues mean square displacements (shown to accurately reproduce crystallographic data) provides a reliable and statistically accurate method to identify crucial folding sites/contacts. This novel strategy is validated against clinical data for HIV-1 Protease. Finally, we compare the spectra and eigenmodes of vibration of natural proteins against randomly-generated compact structures and regular random graphs. The comparison reveals a distinctive enhanced flexibility of natural structures accompanied by slow relaxation times at the folding temperature. The fact that these properties are intimately connected to the presence and assembly of secondary motifs hints at the special criteria adopted by evolution in the selection of viable folds.

I. INTRODUCTION

The backbone structure of globular proteins displays a notable degree of order and organization resulting in secondary motifs such as α -helices and β -sheets and in their optimal arrangement of the constituting secondary motifs into a compact shape. The special neatness and regularity of native conformations impacts on, or rather reflects, several features that are distinctive of naturally occurring proteins^{1,2,3,4}. Indeed, experimental and theoretical studies have shown that native structures conceal a wealth of information about aspects as diverse as native elastic properties, folding rates and key folding stages^{5,6,7,8}. Recent topology-based approaches, which are independent of sequence specificity, have revealed that a schematic, coarse-grained structural description is sufficient to obtain results in remarkable qualitative and even quantitative agreement with known experimental facts.

For example, concerning near-native vibrations, one is entitled to replace the detailed interactions among amino acids which are in contact in the native state with springs acting on effective centroids (usually the C_α atoms)^{5,9}. Topological folding models, on the other hand, try to characterize how the loss of configurational entropy contrasts the progressive establishment of native interactions in a folding process^{3,8,10,11,12,13,14,15}.

In the present study, we focus on a topology-based model that incorporate both the aspects mentioned above. It consists of a beads-and-springs model but, at variance with other approaches, the strength of the effective interaction depends in a deterministic way on the temperature of the thermal bath¹⁶. Since the model is amenable to analytic treatment, it is possible to characterize rigorously both the thermodynamics as well as the vibrational/relaxation dynamics at various equilibrium stages of the folding process (not only near the native state).

The scope of the present study is two-fold. First we examine how the organisation of native contacts impacts on fundamental properties of proteins and, hence, to what extent the knowledge of the contact map can be exploited to predict experimentally verifiable quantities. Our second goal is to repeat the same analysis in the context of generic disordered globular structures. From the comparison of the outcomes we aim at finding clues about the criteria adopted by nature in the selection of viable folds.

The vibrational spectrum at finite temperature allows to determine typical relaxation times which, in turn, correlate with high accuracy with experimental folding rates. This is rather surprising and unexpected since the relaxation time refers to near equilibrium situation whereas the folding process is far from equilibrium. Furthermore, it will be shown that the relaxational dynamics of proteins is very special compared to that of disordered globular structures, or otherwise random graphs. In fact, the natural modes of vibration near the native state involve the protein regions which are important for biological activity¹⁷; the same analysis at finite temperature, when the protein is partially folded, reveals the key sites for the folding process. In addition, the amplitude of vibration of individual amino acids in partially folded states is shown to correlate significantly with experimental B factors.

Finally, the comparative study of analogous static and vibrational properties of disordered compact structures and proteins shows that the latter have very uncommon properties in terms of flexibility and mechanical relaxation times.

These special properties reflect the hierarchical assembly of protein native states¹⁸ and, in particular, can be traced back to the presence and organisation of secondary elements. Hence, they add to the increasing evidence that the emergence of such motifs was promoted by special criteria operated by nature to select viable folds^{2,19,20,21,22}.

The straightforward implementation of concepts presented here, makes the model under consideration a useful tool to characterize the folding properties of a protein, complementing alternative theoretical strategies or more labour-intensive experimental techniques.

II. THEORY

The model under consideration incorporates two features that previous theoretical investigations have proved successful for protein modelling. In spirit, it belongs to the class of Go-models¹⁰, since the energy scoring function introduces a bias in structure space favouring the formation of native contacts. This ensures that the native structure under examination has minimum effective energy. Furthermore, we make use of the observation that, near equilibrium, complicated atomic interactions can be well-reproduced by simple harmonic potentials⁹. The starting point of our analysis is the following effective harmonic Hamiltonian¹⁶ (for its derivation, see Appendix A):

$$H = \sum_{i,j} \mathbf{r}_i L_{ij} \mathbf{r}_j + f(T), \quad (1)$$

where \mathbf{r}_i denotes the distance-vector of site i from its position in the native structure, and f is a term that only depends on the equilibrium temperature. The entries of the symmetric matrix, L , incorporate the elastic forces that act on each residue to restore the native separation with its nearest neighbours in sequence (effect of the peptide bonding) and with other amino acids in interaction in the native state. The peptide bond is modeled by springs that have elastic constants independent of temperature. This reflects the little change of the peptide coupling over the range of temperatures where unfolding/refolding transitions are studied. In addition to this contribution, at variance with previous approaches, the energy scoring-function includes temperature-dependent interactions between the pairs of residues contacting in the native state. The list of such interactions is summarised in the contact map, Δ , whose entries, Δ_{ij} , are 1 if residues i and j are in contact in the native state (i.e. their C_α separation is below the cutoff $c = 7.5$ Å) and 0 otherwise. For simplicity we refer to these temperature-dependent interactions as non-covalent, although they also act on consecutive residues. The strength of such non-covalent springs is calculated self-consistently according to the method described in Appendix A. This makes the model non-linear but still very tractable. When the temperature of the model is zero (this mathematically-convenient idealization corresponds to a physiological temperature where the protein is stable in its native state), all springs have the same strength. As temperature is switched on, this strength is reduced by a deterministic amount that is larger for springs where the largest stretching is observed (see Appendix A).

III. RESULTS AND DISCUSSION

A. Vibrational properties of proteins and disordered structures

At zero temperature, when the non-covalent springs are equally strong and dominate in number over the covalent ones, the model is equivalent to the Gaussian Network Model of Bahar and co-workers^{17,23,24}, which has been widely used to characterize the mobile regions of the native state from the analysis of the normal modes of the structure. These represent the natural oscillations (independent of each other) of a protein and convey information about which regions are more flexible, and how thermal energy is dissipated in order to restore equilibrium (i.e. the native structure). Although atoms in proteins are as tightly packed as in crystalline solids, the vibrational properties of native structures are very different⁵. A notable example is given by the density of eigenvalues of the L matrix, that is the histogram of vibrational frequencies.

This is shown in Fig. 1, where we concentrated on two examples: an individual enzyme, the monomer of the HIV-1 protease, and the average histogram calculated for several instances of two-state folders in Table I. Rather than taking crystalline solids as a reference, we consider several disordered reorganization of the native contacts. The disorder in Δ can be introduced in several ways, the extreme one being a complete reshuffling of Δ . However, it is instructive to consider first the cases when only a modest disorder is introduced by a “conservative” contacts reshuffling that still preserves some fundamental properties of Δ . Successively we shall consider the case of completely disordered maps but with equal connectivity (burial) for each site. It is important to stress that in these two cases of disorder, the Δ

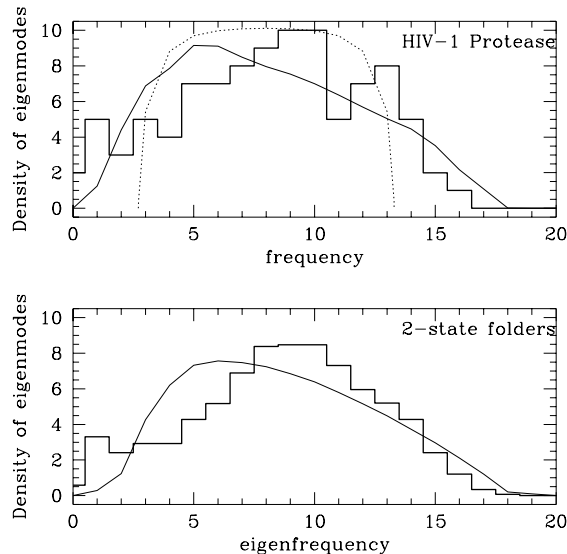


FIG. 1: (top) Density of eigenmodes for (a) HIV-1 Protease (heavy line), (b) average over 3000 conservative reshufflements of HIV-1 PR contact map (light line). The dotted line is the exact density of eigenmodes for a regular graph with $k = 8$ (see text). (bottom) Average density of eigenmodes for the two-state folders of Table 1 (heavy line) and for 100 contact map reshufflements for each of them (light line). Reported data refers to near-native vibrations, corresponding to $T = 0$ in our model.

matrices are not, in general, viable contact maps of any three-dimensional structure. For this reason, we complete our analysis by considering the case of contact matrices of three-dimensional compact self-avoiding structures generated randomly with a computer with the constraint to be as compact as naturally-occurring proteins.

We first consider the mildest case of disorder, i.e. random reshufflements that preserve both the symmetry of Δ and also the protein native burial profile, i.e. the native number of contacts to which each site takes part³. The preservation of the connectivity of each site allows to study the impact of disorder on the vibrational frequency spectrum while keeping burial profiles unaltered. As anticipated above, such randomized contact maps are not necessarily the counterpart of any feasible three-dimensional structure; in fact, a more appropriate view of such matrices is within the framework of graphs^{25,26}, (the nodes and links corresponding to beads and springs, respectively).

A very important difference shown in Fig. 1 is that proteins have a larger number of low-frequency modes of vibration compared to the spectrum of the reshuffled maps. This difference is made more dramatic by considering the spectrum of regular graphs. The term *regular* here refers to the fact that all sites have the same connectivity (burial), k , but the entries of the associated symmetric matrix, Δ are otherwise random²⁷.

This limit case of disorder is important because the average spectrum of such ensemble of matrices has been calculated exactly by McKay²⁸. The density of eigenfrequencies is given by:

$$f(x) = \begin{cases} \frac{k\sqrt{4(k-1)-(x-k)^2}}{2\pi(k^2-(x-k)^2)} & \text{for } |x-k| < 2\sqrt{k-1} \\ 0 & \text{otherwise,} \end{cases} \quad (2)$$

and its distribution is shown in Fig. 1 for the case $k = 8$, corresponding to the average site connectivity (including peptide bonding) in real proteins (when the interaction cutoff is around 7.5 Å).

It appears that the range of vibrational frequencies is severely limited compared to that of real proteins; in fact, the spectrum of such graphs reproduces only the central part of the frequency histogram of proteins. The outlying tails at both low and high frequency are not captured at all. Previous studies have pointed out how such tails reflect the existence of heterogeneity in site connectivity (burial)^{29,30}. This fact, and its implications for the mechanical properties of natural biopolymers are examined in detail in the next section.

B. Localization properties

In a variety of contexts, from the physics of disordered systems to graph theory, spectra have always attracted considerable attention because of the special localization properties of the associated modes. High frequency normal

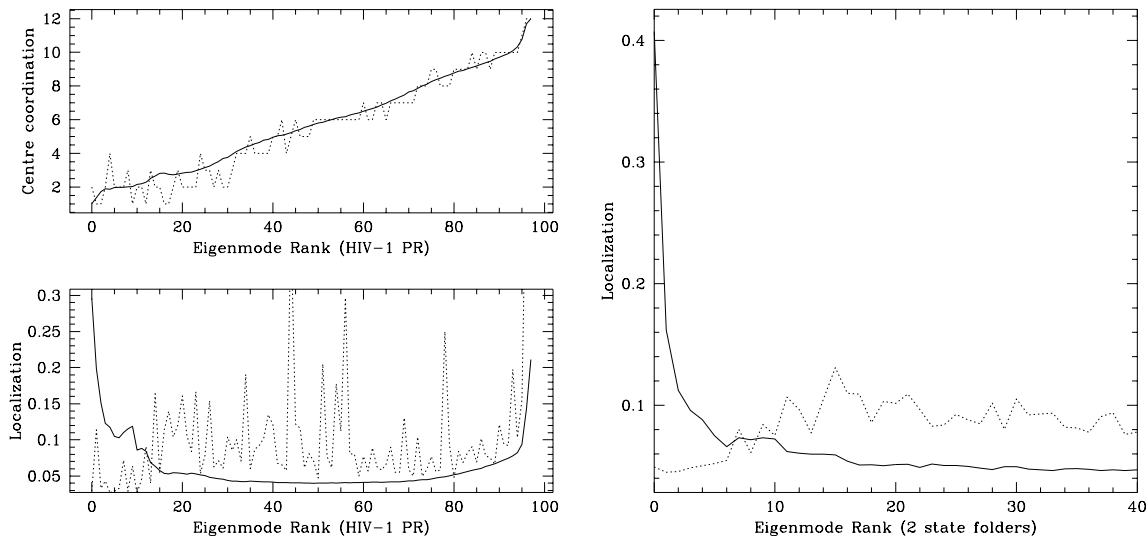


FIG. 2: (top left) Degree of burial (number of native contacts) of sites that are at the center of the various eigenmodes. The eigenmodes are ranked according to increasing vibrational frequency. The centre of an eigenmode is the site where one encounters the largest component (in absolute value). (bottom left) Degree of localization of the eigenmodes. The smooth solid lines pertain to averages over 3000 reshufflings of the protease (monomeric) contact map (but preserving the site connectivity). The dotted line relates to the native state. (right) Degree of localization of the first 40 eigenmodes averaged over the two-state folders of Table 1 (dotted line) and over 100 reshufflements for each of them (solid line).

modes are usually concentrated on sites/regions with high connectivity^{29,30,31,32}. This is intuitive since a larger number of connections leads to an enhanced local stiffness and hence a higher frequency of vibration. Conversely, low frequency modes are centred on sites/regions that having fewer connections than average, are more flexible^{17,29}. This overall picture applies remarkably well to the reshuffled contact maps, as visible in Fig. 2. The plots show that the modes at low [high] frequency are very localised on sites with low [high] connectivity (burial). The degree of localization of a normalized eigenmode of vibration, $\{v\}$ is defined as $\sum_j |v_j|^4$ (see eg.³⁰).

It is now interesting to turn to the case of proteins. Fig. 2 shows that high-frequency modes are, as before, highly localised on heavily buried sites. Notice that the highly localized states are not limited to the upper edge of the spectrum. The picture, however, changes for low-frequency modes, which appear to be significantly more delocalised than for the reshuffled case. This denotes a degree of flexibility that is significantly larger than randomly connected graphs (yet with the same burial profile!). This is not a peculiar feature of the HIV-1 Protease monomer, but is more general, as illustrated in the right panel of Fig. 2 displaying averages taken over the two-state folders of Table 1 and their reshufflements. The averages in Fig. 2 are reported only for the 40 slowest modes, which cover a similar range of frequencies across the proteins of Table 1. The inhomogeneity of the lengths of such proteins prevents from taking straightforward averages over the whole frequency range.

Several previous investigations of normal modes and spectra of proteins^{33,34,35,36,37,38,39,40,41,42} had already noted the existence and utility of low-frequency modes in proteins, arguing that the slowly moving regions are the natural candidates for biological functions involving structural rearrangements. It is important, however, to note that also random graphs have low-frequency vibrations; the novel message of Fig. 2 is that in proteins, the slowly-moving regions are much more extended. This special property, which does not depend on the burial profile, must result from the special organization of native contacts which provides a remarkable degree of flexibility. This, in turn, is associated with a rate of thermal energy dissipation that is slower compared to disordered graphs. The natural measure for the limiting rate at which mechanical excitations decay is, in fact, given by the smallest frequency (eigenvalue) of L . Equivalently, the slowest vibrational relaxation (decay) time in the system, which we shall denote as λ_0 , is given by the inverse of the smallest vibrational frequency, ω_0 .

The immediate cause for this further difference is simply described in terms of graph properties²⁵. There is a well-defined relationship between the slowest relaxation time and the average contact-diameter (meaning the average number of native contacts that have to be traversed to go from an arbitrary site to another). This relation is neatly visible in the bottom plot of Fig. 3, which displays results for the distinct proteins of Table I, and an equal number of their reshufflements.

It is important to see that, among all proteins, the ones with many local contacts (all- α family) tend to be at

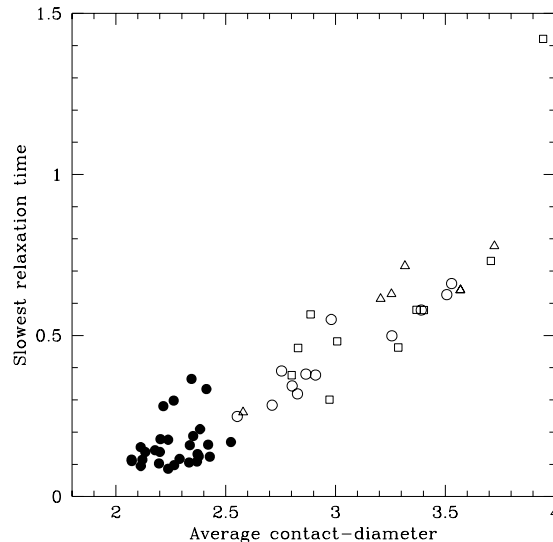


FIG. 3: Scatter plot of the slowest native relaxation times ($T = 0$) versus the average native contact diameter. The data pertain to the proteins in Table 1 (open symbols) and an equal number of computer-generated disordered compact structures with same length distribution (filled circles). The open triangles, square and circles denote proteins belonging to the α , β and $\alpha\beta$ families respectively.

one end of the scatter plot, while proteins belonging to the all- β family are closer to the case of reshuffled contact maps. Finally, to complete our investigation we also considered disordered three-dimensional structures. These are expected to have a behaviour that is intermediate between that of real proteins and the random reshufflements. Also in this case the relaxation time of proteins is larger. Within our model this is best understood working at finite temperature rather than at $T = 0$. This is illustrated in Fig. 4 where we considered $T = 2T_F$, with T_F given by the folding transition temperature at which the peak in the specific heat is observed¹⁶. The reason for this is that in our model, at low temperature, non-covalent interactions prevail over the peptide bonding. In simpler terms, residues vibrate around their native positions, but there is no information about the rigidity of the peptide bond. This leads to an ambiguity about the correct succession of residues and, as a consequence, it blurs the distinction between ordered and disordered three-dimensional structures (but the one with random graphs is still neatly discernible). Of course, also in the opposite limit of very high temperature, where virtually all native contacts are broken, there is no difference between the behaviour of proteins and compact three-dimensional structures. These ambiguities are resolved at moderate temperatures, where both the peptide interactions and non-covalent ones are important. It is apparent that protein structures have systematic higher relaxation time than random, three-dimensional decoys (see Fig. 4).

This can be understood from the fact that the establishment of a few disordered contacts, very rapidly makes the structure rigid, and less susceptible to further rearrangements. The hierarchical organization of contacts in proteins, in terms of secondary motifs further arranged in the tertiary structure, is responsible for the enhanced flexibility visible in Figs. 3 and 4. In fact, the relaxation times of *isolated* secondary motifs, both α and β , of equal length is nearly the same and, again, much higher than a corresponding random reshuffling. This is illustrated in Figs. 5 and 6. From these facts it is tempting to speculate that α - and β -like motifs are the configurations that, for a given burial profile, have the largest relaxation times. This is particularly intuitive in the case of helices since their periodicity (modulus boundary effects) is immediately associated to the presence of slowly-decaying excitations. It is also interesting to examine the implications of the fact that, in compact globular proteins, the individual secondary motifs are hold together by a network of other contacts, usually non-local. As a consequence, the whole structure is more rigid than the individual building blocks (the motifs). This interpretation is supported by Figs. 5 and 6, where one can see that the slowest relaxation time of individual motifs (equal to 0.8 in our units) is effectively an upper limit for the relaxation time for the whole protein structures. Due to the relative locality of tertiary contacts, all- α proteins are almost as flexible as the α -motifs themselves, while all- β structures have a much augmented rigidity. It is important to notice that the relaxation time of these motifs is equal to the largest relaxation times observed in entire protein structures. This is consistent with the interpretation that the relaxation time of the highly flexible secondary motifs is an upper limit for the relaxation time of the entire protein (that is lowered by the non-local interactions responsible for the tertiary assembly which, in fact provide the mechanical stiffness).

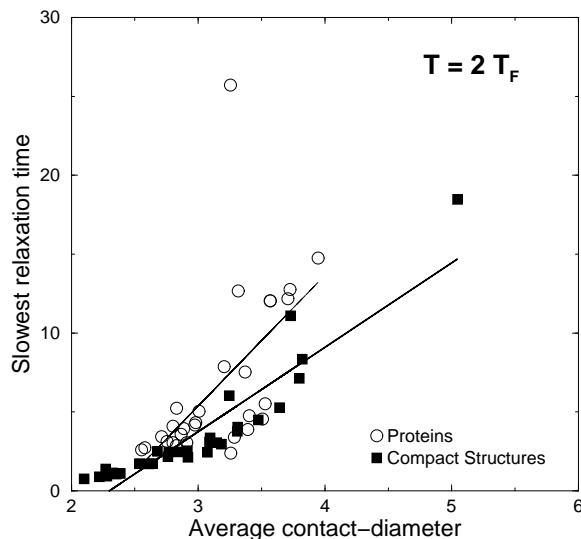


FIG. 4: Scatter plot of the slowest relaxation times at $T = 2 T_F$ versus the average native contact diameter. The data pertain to the proteins in Table 1 (open symbols) and an equal number of computer-generated disordered compact structures with same length distribution (filled circles).

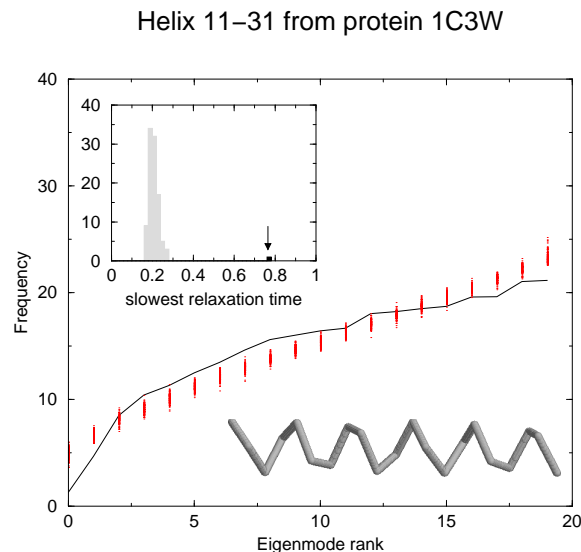


FIG. 5: Frequency spectrum at $T = 0$ of helix 11-31 from protein 1c3w (continuous line) and of 100 conservative random reshufflements of its contact map (dots). The inset displays the histogram of the slowest relaxation times, λ_0 for the reshuffled maps and the original helix (indicated by the arrow).

C. Folding rates

In this subsection we shall explore the intimate connection between the relaxation time of slow eigenmodes of protein structures in thermal equilibrium and the protein folding rate. In one of the best known (and earliest) studies of folding times, Levinthal pointed out how typical folding times are remarkably short compared to the expected time required to find the native state in a random exploration of the whole conformation space, Γ . The solution to this apparent paradox is in the fact that the structures in Γ will not have the same weight (due to energetic and entropic effects). Therefore, the route of a protein from its initial state to the native one does not occur in a flat free-energy landscape, but in one that is biased towards the native state. This bias arises from several factors, including the interaction potentials between amino acids, solvophobic effects, configurational entropy, etc.

The overall shape of the biased landscape in structure space will depend both on the native structure itself, and

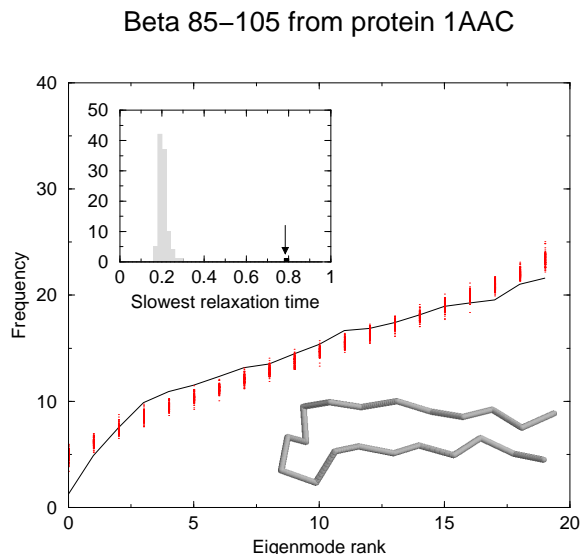


FIG. 6: Frequency spectrum at $T = 0$ of beta sheet 85-105 from protein 1aac (continuous line) and of 100 conservative random reshufflements of its contact map (dots). The inset displays the histogram of the slowest relaxation times, λ_0 for the reshuffled maps and the original sheet (indicated by the arrow).

on the detailed chemical interactions. Theoretical and experimental studies have shown that the main features are typically determined by native state topology. Different native shapes will then be associated with landscapes that, despite being biased towards the native conformation, may have significant differences in terms of numbers of metastable minima, height of the barriers between them etc. The corrugation of the landscape will undoubtedly affect the folding rate. The relaxation time of a structure in thermal equilibrium provides a measure of the average ruggedness of the landscape. In the case of a short relaxation time the thermal energy of the solvent molecules impinging in the structure is dissipated rapidly and the number of distinct conformations visited per unit time will be small. Thus, the native state is reached with greater difficulty if, during the folding process, the partially-formed structures have smaller relaxation times (in equilibrium). In other words it is not advantageous for a protein to dissipate energy too rapidly (i.e. short relaxation time), because this hinders the structural rearrangements necessary to fold in the native conformation. Combining this with the previous indication that secondary motifs have the slowest relaxation times (for given length and burial profile), suggests that their early formation and later assembly makes the folding process occur under very low energy dissipation. On the other hand one expects that protein structures have been also selected for a fast and efficient folding whereas generic compact structures have not these properties. Thus it is plausible that folding and relaxation times, at a temperature where the protein starts to fold, are somewhat related. This is not anymore the case for random compact structures where the relaxation is fast and correspondingly the folding is slow.

In agreement with this picture, we have found a notable correlation (see Fig. 7) between the experimental folding rates, $\ln K_F$ and the slowest relaxation rate, λ_0 (in dimensionless units) which dominates the long-time relaxation kinetics in equilibrium. At temperatures much larger than the folding temperature, T_F (identified as the temperature at which the peak of the specific heat is observed), the relaxation time conveys little information about the folding rate, since virtually no contacts are formed, this is true also at low T , where it measures only the rate of thermal dissipation of the fully-folded native structure.

The highest correlation is observed at finite temperatures, higher than T_F (see Fig. 7). Although we believe that the precise location of the peak of the correlation may be sensitive to the model details, this result is plausible since it is above the folding transition that the significant search in conformation space occurs. The correlation coefficient at the optimal temperature is as high as $r = 0.79$. It is straightforward to assess its statistical significance by computing the probability to have observed a value higher than this if the relaxation rates were picked randomly from a normal distribution (the mean and spread of the distribution do not affect the linear correlation coefficient). This probability turns out to be equal to $t = 4 \cdot 10^{-5}$, which denotes the high significance of the prediction. These results adds to previous studies where folding rates were predicted with analogous level of significance on the basis of contact locality⁶ or different topologic indicators (such as the cliquishness) based on a graph-theoretical description of a protein's non-bonded interactions²⁶.

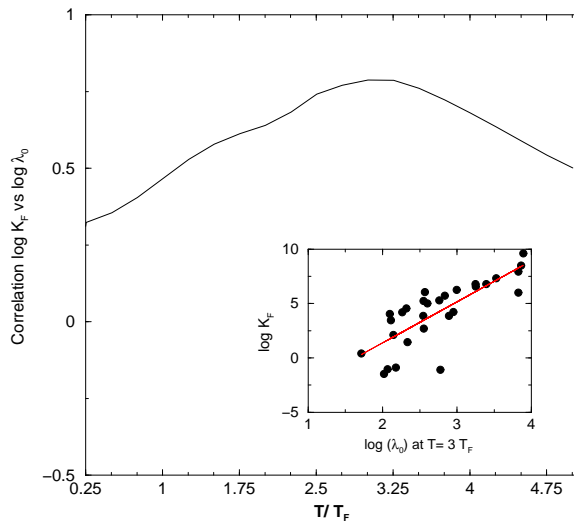


FIG. 7: Linear correlation coefficient between the logarithm of the theoretical relaxation time, $\log \lambda_0$, and experimental folding rates for the proteins folding via a two-state mechanism (Table 1). The inset shows the scatter plot of the actual theoretical and experimental values at a temperature close to where the best correlation, $r = 0.79$ is observed.

D. B factors

The choice of a simple Gaussian Network Model to investigate the biological function of proteins has been motivated by a striking qualitative agreement between the experimental B factors (or temperature factors) measured in X-ray diffraction experiments and the mean square residue displacement calculated theoretically from the expression^{17,24,43}:

$$B_i^{\text{theory}} \propto \sum_k \frac{1}{\omega_k} |v_i^k|^2 \quad (3)$$

where i is the residue index, k runs over all non-zero frequency modes and ω_k [$\{v\}$] denotes the k th eigenfrequency [eigenmode], respectively.

In this section we perform an analysis of the correlation between the theoretical and experimental B factors, aimed at investigating the agreement between thermal fluctuations calculated in the present model and the overall temperature factors in resolved crystal structures. We stress that in our model, both eigenfrequencies and eigenmodes are temperature-dependent.

We begin our analysis by considering the $T \rightarrow 0$ limit of our model, that corresponds to the GNM studied in References^{23,24,37}.

We analyzed 30 protein structures, all obtained in X-ray diffraction experiments, of different size (up to about 200 amino acids). The proteins, listed in Table 2, are chosen among the monomeric representatives of distinct structural classes obtained from high-resolution data⁴⁴. Thermal fluctuations for each amino acid were compared with the corresponding temperature factor reported for the CA atoms in the PDB file⁴⁵. The mean value of the correlation coefficient is 0.62 ± 0.13 (it should be emphasized that this average is the simple arithmetic mean without any length-dependent reweighting of the data). Although we obtained a remarkable agreement with experimental data for several proteins (correlation coefficients larger than 0.75 for proteins with nearly 200 residues), in some rare instances the correlation was around 0.4 (see Table 2). It must be borne in mind, however, that such correlations are never trivial, since they are measured over the entire protein length. Accordingly, in the worst cases, the probability to observe higher correlations than the measured ones, through a random gaussian choice of the theoretical B 's is less than 0.03 %. The agreement with temperature factors is therefore statistically relevant, although does not have the same quality for all crystal structures. It is important to remark that the crystallographic B -factors are not obtained by direct measurement, but from a suitable parametric fit of the measured diffraction pattern. In unfavourable conditions (affected also by crystallographic resolution), the fit may be significantly underdetermined and reliable data can be obtained only imposing additional constraints on the B factors (such as their smooth variation along the main- or side-chains). Inspection of the PDB files for which the worst correlations are seen have revealed that, indeed, those proteins lacked the B -factor smoothness. Another possible source of discrepancy between theoretical and experimental data is the fact that we neglected the proximity effect of the surrounding proteins in the crystal

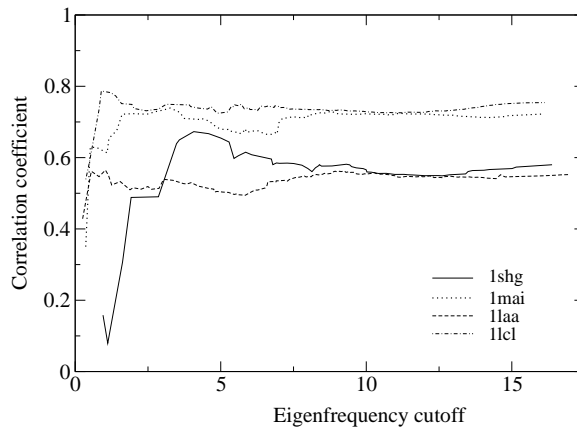


FIG. 8: Correlation coefficients for thermal fluctuations obtained truncating the sum over eigenmodes up to the cutoff eigenfrequency reported on the x axis.

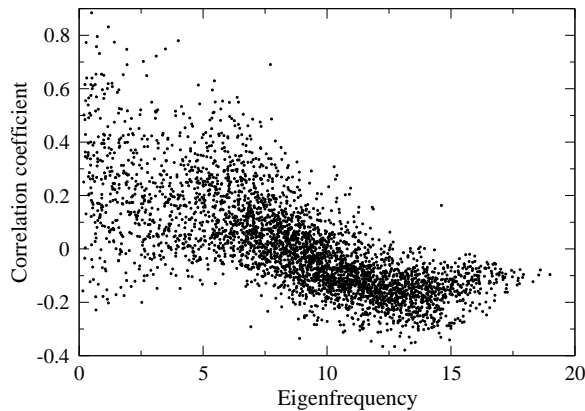


FIG. 9: Correlation coefficients between single eigenmodes amplitudes and experimental B factors as a function of their corresponding eigenfrequencies. The points refer to all eigenmodes of the X-ray structures of Table 2.

structure. Hence, it is possible that some parts of the protein (and notably those experiencing a pronounced freedom of movement) experience a reduction of mobility due to the presence of neighbouring proteins.

It is fruitful to examine also in this context the distinct contribution to the sum in (3) of the different eigenmodes. In fact, thermal fluctuations are calculated as weighted sums of single eigenmodes, the weights being reciprocal of the corresponding eigenfrequencies. We have extended our analysis to the single vibrational eigenmodes. In Fig. 8, we plot the coefficient of the linear correlation between the experimental B -factors of four proteins against the theoretical estimates of eqn. 3, where the sum over the r.h.s. includes only eigenmodes with frequency lower than a pre-assigned cutoff value.

We notice that the correlation coefficient saturates to a maximum value for a typical cutoff frequency of 6 (in dimensionless units). This result was found for virtually all the protein structures we considered. It appears that much of the information on temperature factors indeed comes from the slowest eigenmodes, i.e. those corresponding to the lowest eigenfrequencies. This reinforces the hypothesis on the relevance of slow modes to the biological function of the protein¹⁷. It may be argued that this is an expected result, since all eigenmodes have been weighted with the reciprocal of the eigenfrequencies. However, fast eigenmodes do not contribute significantly to the temperature factors, even in the absence of any weight. Fig. 9 shows the linear correlation coefficients obtained by correlating the experimental B values with the contribution to the sum of Eq. 3 of each individual eigenmode.

The majority of positive correlations are found in the region of slowest eigenmodes (eigenfrequencies up to 6), while there is a negligible correlation, on average for middle eigenfrequencies, and a weak anti-correlation for fast eigenmodes (eigenfrequencies larger than 12). The anti-correlation of the experimental B -factors with the square-amplitudes profile of fast eigenmodes is in agreement with the graph theoretical prediction of a localization of the

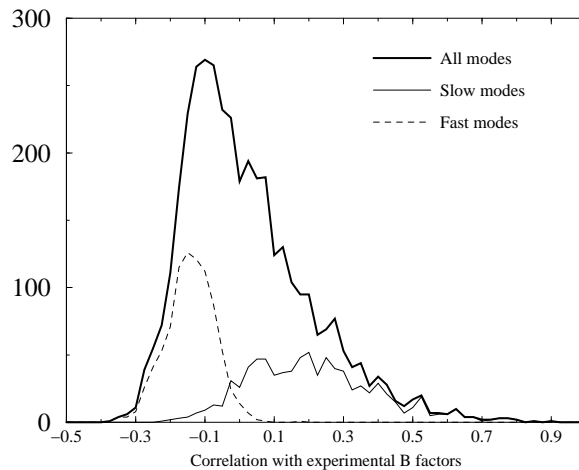


FIG. 10: Histograms of correlation coefficients of single eigenmodes amplitudes and experimental B factors. Positive correlations come from slow modes, negative from fast modes.

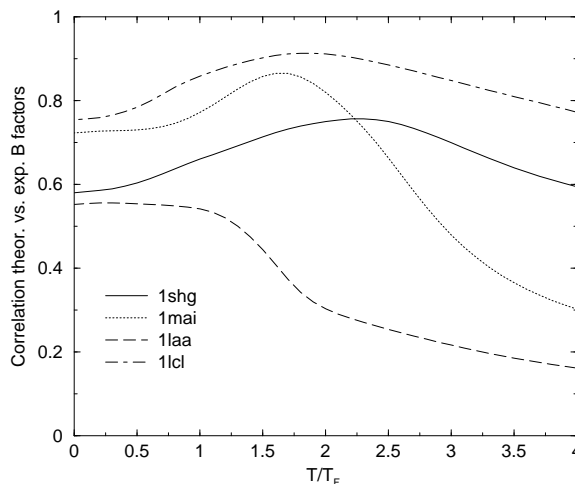


FIG. 11: Correlation between theoretical and experimental B factors as a function of temperature.

fastest eigenmodes in nodes of higher connectivity. These nodes are less mobile in the protein structure and hence associated with smaller B values. Furthermore, since all eigenmodes are orthogonal, the sites whose vibrational amplitude is large in the slowest eigenmodes, will not be very mobile in the fastest ones, and viceversa. A quantitative support to this argument is provided in figure 10, where we report the projection of figure 9 on the correlation axis.

Following this analysis we can conclude that rough estimates of temperature factors for structures obtained by X-ray diffraction experiments, can be obtained as weighted sums conveniently restricted to the slowest vibrational eigenmodes. These eigenmodes indeed cooperate to generate much of the fluctuation pattern of the protein structure, while intermediate modes have little influence and fast modes could be safely excluded from the sum, since they contribute to raise the mobility of highly connected nodes.

Finally, we observe that the theoretical B 's carry a non trivial dependence on temperature through the eigenmodes (due to the temperature dependence of matrix L). Fig. 11 summarises the behaviour of the correlation with experimental data against temperature for four representative proteins. It can be seen that, typically, by working at a temperature around $2T_F$ the correlation with experimental data can be increased significantly. As visible, an exception to this trend is given by the few proteins which already have a poor correlation at $T = 0$.

We have considered also the case of NMR proteins, for which accurate relaxation measurements can directly probe the mobility of local portions of the protein thus providing an *effective* B factor. Strikingly, the correlation between the theoretical and the experimental B factors observed in this situation was systematically higher than for the X-ray resolved counterparts, as can be ascertained from Table 2. The mean correlation at zero temperature was, in fact, 0.76 ± 0.04 , with a net improvement over the X-ray case (0.62 ± 0.013). It would be tempting to conclude that

this improved agreement is due to the more direct way with which NMR experiments can address local vibrational amplitudes. However, due to the insufficient annotation of PDB files of some NMR-resolved structures, it is not always possible to ascertain whether the reported data follow from precise relaxation measurements or from an *a posteriori* analysis of the various model structures compatible with measured distance-constraints.

Due to the insufficient annotation of PDB files of some NMR-resolved structures, it is not always possible to ascertain when the reported temperature factors are valid indicators of the actual mobility of residues.

E. B factors and key sites

The analysis of the mobility, in thermal equilibrium, of different protein residues carries significant information about sites that are important in the folding process. We illustrate this important application for the case of the HIV-1 Protease. This enzyme represents an ideal benchmark due to the vast number of clinical studies thanks to which comprehensive tables of key mutating sites have been compiled^{46,47,48,49,50,51}. Molecular dynamics studies applied to topological folding models of the protease have shown that the key mutating sites are involved in contacts that act as limiting steps for the folding process⁸.

One attempt to describe/predict this crucial set of amino acids from the analysis of normal modes was carried out in Refs.^{23,24,37} with the aid of the Gaussian Network Model (to which our model reduces when $T = 0$), who pointed out that high frequency modes are localised close to key mutating sites³⁸. Our results, especially those of Fig. 2, support the view that the sites where the high frequency modes concentrate are paramount for native stability; in fact they are among the least exposed ones. However, this property is only related to the native structure, and does not imply that the same sites play the leading role in overcoming the folding rate-limiting steps.

A more direct strategy would be to determine the handful of contacts that form cooperatively at, or in the neighbourhood of, the folding transition temperature. The formation of such contacts, which has an all-or-none character, is expected to constrain significantly the mobility of the residues involved in their establishment. This scheme, which has been confirmed *a posteriori* in simplified folding models of the HIV-1 PR and prion^{8,52}, can be naturally adopted in the present case. In fact, a natural and convenient measure of the degree of spatial constraint of a given site is provided by the associated B-factor. Thus, near the folding transition temperature, one expects that the key sites have nearly native like values for the B factors, while other residues will have much larger fluctuations than in the native state. Therefore, one may identify the key sites as those with small values of B or small derivatives of B with respect to temperature. It turns out that both these criteria work well, as illustrated in Fig. 12. Among the top 13 sites ranked according to the smallness of B factors there are 5 key residues: 32,33,77,84,30. In the top 13 sites ranked according to the derivative of B there is an additional key site, namely residue 82. The probability to observe at least these many matches if we had chosen the sites randomly would have been 3 % and 0.5 % respectively in the two cases. It must be stressed that the present strategy to identify key sites exploits the information on native topology in a non-trivial manner avoiding, for example, the pitfall of selecting the most buried sites as the key ones. In fact, to collect the same number of correct matches found before, one needs to retain about twice as many burial-ranked sites than for the B-factor-ranked case. We have verified that this conclusion holds for all interaction cutoffs in the range 6.5-8 Å. This very good statistical validation shows that the physically appealing identification of the key sites through normal modes analysis can be fruitfully applied in contexts of high practical importance.

IV. CONCLUSIONS

We have focused on the characterization of both the folding process and equilibrium physical properties of natural proteins through the normal modes analysis of a suitable topological model. Previous investigations of normal vibrations around the native state have proved a valuable tool to describe the large scale motion of proteins and obtain clues about their biological functionality.

Although we also focus on specific protein instances, such as the HIV-1 protease, our scope is more directed at finding some general characteristics of proteins' dynamics in thermal equilibrium (at various temperatures) that distinguish these biopolymers from a randomly compact polymer. This comparison has a two-fold objective: one of theoretical interest, the other more practical.

From the other of theoretical biophysics, the identification of features that are unique (and common) to proteins provides clues about the special evolutionary criteria that have promoted the selection of the wide repertoire of naturally-occurring proteins yet using only a limited number of fold families^{4,19,20}. In the detailed account provided here we have shown that proteins are very flexible and have long relaxation times, in thermal equilibrium, compared to globular polymers. In turn, the relaxation time of partially folded states is shown to have a significant correlation with experimental folding times (r can be as high as 0.79). We give a quantitative account of the intimate dependence

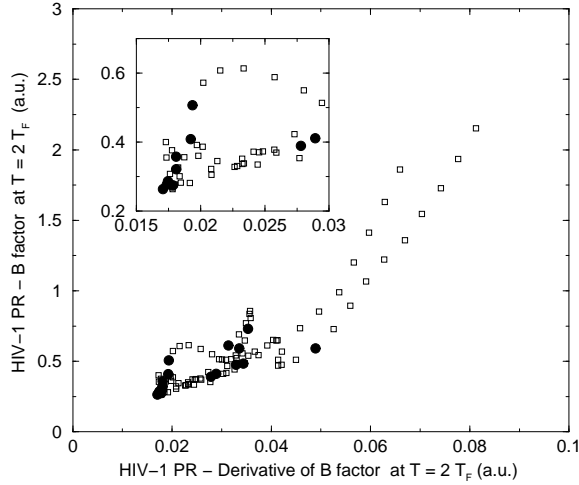


FIG. 12: Scatter plot of B-factors and their temperature derivative for the sites of HIV-1 PR monomer. The key sites known to cause resistance to protease-inhibiting drugs are highlighted.

of the relaxation rates with native state topology; thereby providing a novel additional support to the influence of native-state topology over folding rate. It is also found that high-frequency modes involve as many sites in natural proteins as in disordered structures. Despite this, the structural regions involved in slow motions are much more extended in proteins. Without this property (common to the few tens of proteins considered here) it would probably be impossible for a protein to carry out the articulated mechanical tasks necessary for biological functionality^{38,39,40,41}. The direct investigation of the vibrational properties of individual secondary motifs has shown that their presence and organization are distinctive features of protein structures. This observation adds to previous evidence according to which the ubiquity of secondary motifs in real proteins is due to the very special properties that they confer both to the native state and to the folding process.

From a more practical point of view, the knowledge of how these "special features" have arisen through the selection of certain viable native shapes, can be used as a predictive tool. In particular, the straightforward deterministic analysis of the topologic folding model adopted here allows to predict folding rates with high statistical significance. A further important application is in the "a priori" determination of the B factors that are essential in the refinement and validation of protein structures resolved by X-ray and NMR. To the best of our knowledge, no previous studies exist where a quantitative comparison of theoretical and experimental B factors has been attempted. A by-product of the analysis of B factors of partially folded states is the identification of the sites (or contacts) that lock into their relative native position at early stages of the folding process. Taking the case of HIV-1 PR as a reference, we have shown that such sites are among those that are known to be involved in rate-limiting steps of the folding process. Therefore, within this single simple framework it is possible to model various aspects of the folding process and other equilibrium properties obtaining a thorough protein characterization that is consistent with available experimental results.

This work was supported by INFM and MURST cofin 2001. We are indebted to Jayanth Banavar, Burak Erman, Dorian Lamba and Henriette Molinari for many stimulating discussions.

APPENDIX A: METHODS: ANALYTICAL CHARACTERIZATION OF THE MODEL

The simplified energy functional used to characterize the equilibrium or folding properties of a target structure, Γ is:

$$H = \frac{K \cdot T}{2} \sum_{i=1}^{N-1} (\mathbf{r}_i - \mathbf{r}_{i+1})^2 + \frac{1}{2} \sum_{i \neq j} \Delta_{ij}^{\Gamma} [(\mathbf{r}_i - \mathbf{r}_j)^2 - R^2] p_{ij} \quad (\text{A1})$$

where \mathbf{r}_i denotes the distance-vector of the i th C_{α} from its position in the native structure, Γ (assumed to be N residues long). K is the strength of the peptide bonds, and T is the absolute temperature (incorporating the Boltzmann constant). Δ^{Γ} is the contact matrix, whose element Δ_{ij}^{Γ} is 1 if residues i and j are in contact in Γ (i.e. their C_{α} separation is below a cutoff c . (in this study $c = 7.5 \text{ \AA}$) and 0 otherwise. The matrix Δ_{ij}^{Γ} along with the

native C_α coordinates encodes the topology of the protein. In standard off-lattice approaches, the interaction $V(d)$ between non-bonded amino acids at a distance d , is taken to be a square well potential, or some type of Lennard-Jones interaction. Our choice in Eq. (A1) is a sort of “harmonic well” which, while being physically sound and viable, is suitable for a self-consistent treatment, as explained below.

The temperature-dependent term p_{ij} is the probability that the separation of amino acids i and j fall within a distance R of the native separation. Therefore R plays the role of an effective outer rim of the quadratic potential well and can be set to a few Angstroms ($R = 3 \text{ \AA}$ in the present study) to reflect the fact that, when the separation of two residues exceeds substantially the native one their interaction is negligible.

The simple quadratic form of Hamiltonian in Eq. (A1) allows to determine exactly the p_{ij} ’s from the self-consistent relation:

$$p_{ij} = \langle \Theta(|\mathbf{r}_i - \mathbf{r}_j|^2 - R^2) \rangle. \quad (\text{A2})$$

where $\Theta(x)$ is the unitary step function and the brackets denote the thermal averaging under the action of Hamiltonian A1, that depends on p_{ij} as well. Operatively, one starts from a trial choice of the p_{ij} , which is used to determine a new set of parameters through eqn. (A2). Convergence is obtained in a few tens of iterations at any temperature. Now in such self consistent approach the problem is fully solved and all equilibrium or dynamical quantities can be calculated exactly by evaluating analytical expressions. At $T = 0$ the model correctly assigns the lowest energy to the native structure (all p_{ij} ’s equal to 1). Upon increasing the temperature, each interacting pair will have increasing mutual separation (in modulus) and correspondingly, the p_{ij} ’s will decrease to reflect the milder binding. In the limit $T \rightarrow \infty$ all p_{ij} ’s tend to 1. Simple algebraic operations allow to recast the self-consistent energy function in the following form:

$$\mathcal{H} = \sum_{ij} \mathbf{r}_i L_{ij} \mathbf{r}_j - \frac{1}{2} \sum_{ij} \Delta_{ij}^\Gamma R^2 P_{ij} \quad (\text{A3})$$

where

$$L_{i,j} = \begin{cases} K \cdot T (2 - \delta_{i,1} - \delta_{i,N}) / 2 + \sum_l \Delta_{i,l}^\Gamma P_{i,l} & \text{for } i = j \\ -P_{i,j} \Delta_{i,j} + K \cdot T (-\delta_{i,j+1} - \delta_{i,j-1}) / 2 & \text{for } i \neq j. \end{cases} \quad (\text{A4})$$

While the present form of the model does not accurately describe the effects of self-avoidance, it nevertheless ensures that the native state is the true ground state and satisfies all the steric constraints. The connectedness of the chain, as well as its entropy, are captured in a simple but non-trivial, manner. The most significant advantage of the model is that it can be used to explore both the equilibrium thermodynamics and the relaxational dynamics without being hampered by inaccurate or sluggish dynamics.

-
- ¹ D. A. Baker, Nature **405**, 39 (2000).
² A. Maritan, C. Micheletti, A. Trovato, and J. R. Banavar, Nature **406**, 287 (2000).
³ C. Micheletti, J. R. Banavar, A. Maritan, and F. Seno, Phys. Rev. Lett. **82**, 3372 (1999).
⁴ J. Banavar, A. Maritan, C. Micheletti, and A. Trovato, Proteins: Structure Function and Genetics **in press** (2002).
⁵ D. ben Avraham, Physical Review B **47**, 14559 (1993).
⁶ K. W. Plaxco, K. T. Simons, and D. Baker, J. Mol. Biol. **277**, 985 (1998).
⁷ H. S. Chan, Nature **392**, 761 (1998).
⁸ F. Ceconi, C. Micheletti, P. Carloni, and A. Maritan, Proteins: Structure Function and Genetics **43**, 365 (2001).
⁹ M. M. Tirion, Physical Review Letters **77**, 1905 (1996).
¹⁰ N. Go and H. A. Scheraga, Macromolecules **9**, 535 (1976).
¹¹ O. V. Galzitskaya and A. V. Finkelstein, Proc. Natl. Acad. Sci. USA **96**, 11299 (1999).
¹² V. Munoz, E. R. Henry, J. Hofrichter, and W. A. Eaton, Proc. Natl. Acad. Sci. USA **95**, 5872 (1999).
¹³ E. Alm and D. Baker, Proc. Natl. Acad. Sci. USA **96**, 11305 (1999).
¹⁴ D. K. Klimov and D. Thirumalai, Proc. Natl. Acad. Sci. USA **97**, 7254 (2000).
¹⁵ C. Clementi, H. Nymeyer, and J. N. Onuchic, J. Mol. Biol. **298**, 937 (2000).
¹⁶ C. Micheletti, J. Banavar, and A. Maritan, Phys. Rev. Lett. **87**, DOI:088102 (2001).
¹⁷ I. Bahar, A. R. Atilgan, M. C. Demirel, and B. Erman, Physical Review Letters **80**, 2733 (1998).
¹⁸ R. L. Baldwin and G. D. Rose, Trends in Biochemical Sciences **24**, 26 (1999).

- 19 M. Denton and C. Marshall, *Nature* **410**, 417 (2001).
- 20 C. Chothia, *Annu. Rev. Biochem.* **53**, 537 (1984).
- 21 H. S. Chan and K. A. Dill, *J. Chem. Phys.* **92**, 3118 (1990).
- 22 N. D. Socci, W. S. Bialek, , and J. N. Onuchic, *Phys. Rev. E* **49**, 3440 (1994).
- 23 I. Bahar, A. R. Atilgan, and B. Erman, *Folding and Design* **2**, 173 (1997).
- 24 T. Haliloglu, I. Bahar, and B. Erman, *Physical Review Letters* **79**, 3090 (1997).
- 25 B. Bollabas, *Random Graphs* (Academic, London, 1985).
- 26 C. Micheletti, SISSA preprint pp. <http://xxx.lanl.gov/ps/cond-mat/0202090> (2001).
- 27 R. Merris, *Lin. Alg. Appl.* **197**, 143 (1994).
- 28 B. D. McKay, *Lin. Alg. Appl.* **40**, 203 (1981).
- 29 R. Monasson, *Eur. Phys. J.* **B 12**, 555 (1999).
- 30 G. Biroli and R. Monasson, *J. Phys.* **A 32**, L255 (1999).
- 31 P. W. Anderson, *Physical Review* **109**, 1492 (1958).
- 32 P. W. Anderson, *Reviews of Modern Physics* **50**, 191 (1978).
- 33 I. Bahar, A. R. Atilgan, R. L. Jernigan, and B. Erman, *Proteins: Structure Function and Genetics* **29**, 172 (1997).
- 34 B. Lustig, I. Bahar, and R. L. Jernigan, *Nucleic Acids Research* **26**, 5212 (1998).
- 35 I. Bahar, A. Wallqvist, D. G. Covell, and R. L. Jernigan, *Biochemistry* **39**, 1067 (1998).
- 36 I. Bahar and R. L. Jernigan, *Journal of Molecular Biology* **281**, 871 (1998).
- 37 R. L. Jernigan, M. C. Demirel, and I. Bahar, *International Journal of Quantum Chemistry* **75**, 301 (1999).
- 38 I. Bahar, B. Erman, R. L. Jernigan, A. R. Atilgan, and D. G. Covell, *Journal of Molecular Biology* **285**, 1023 (1999).
- 39 T. Haliloglu and I. Bahar, *Proteins* **37**, 654 (1999).
- 40 I. Bahar and R. L. Jernigan, *Biochemistry* **38**, 3478 (1999).
- 41 O. Keskin, I. Bahar, and R. L. Jernigan, *Biophysical Journal* **78**, 2093 (2000).
- 42 A. R. Atilgan, S. R. Durell, R. L. Jernigan, M. C. Demirel, O. Keskin, and I. Bahar, *Biophysical Journal* **80**, 505 (2001).
- 43 B. Erman, preprint (2002).
- 44 C. Micheletti, F. Seno, and A. Maritan, *Proteins: Structure Function and Genetics* **40**, 662 (2000).
- 45 F. C. Bernstein, T. F. Koetzle, G. J. Williams, E. E. M. Jr, M. D. Brice, J. R. Rodgers, O. Kennard, T. Shimanouchi, and M. Tasumi, *Journal of Molecular Biology* **112**, 535 (1977).
- 46 J. H. Condra et al., *Nature* **374**, 569 (1995).
- 47 P. J. Ala, E. E. Huston, R. M. Klabe, P. K. Jadhav, and P. Y. S. L. and C. H. Chang, *Biochemistry* **37**, 15042 (1998).
- 48 S. Gulnik, J. W. Erickson, and D. Xie, *Vitam Horm.* **58**, 213 (2000).
- 49 A. Wlodawer and J. W. Erickson, *Annu Rev Biochem* **62**, 543 (1993), and references therein.
- 50 P. Reddy and J. Ross, *Formulary* **34**, 567 (1999).
- 51 M. Tisdale et al., *Antimicrob. Agents Chemother.* **39**, 1704 (1995).
- 52 G. Settanni, T. Hoang, C. Micheletti, and A. Maritan, SISSA preprint pp. <http://xxx.lanl.gov/ps/cond-mat/0201196> (2002).
- 53 A. Viguera, J. Martinez, V. Filimonov, P. Mateo, and L. Serrano, *Biochemistry* **33**, 2142 (1994).
- 54 G. S. Huang and T. G. Oas, *Biochemistry* **34**, 3884 (1995).
- 55 R. E. Burton, G. S. Huang, M. A. Daugherty, P. W. Fullbright, and T. G. Oas, *J. Mol. Biol.* **163**, 311 (1996).
- 56 B. B. Kragelund, C. V. Robinson, J. Knudsen, C. M. Dobson, and F. M. Poulsen, *Biochemistry* **34**, 7217 (1995).
- 57 B. B. Kragelund, P. Hojrup, M. S. Jensen, Schjerling, E. Juul, J. Knudsen, and F. M. P. FM, *J. Mol. Biol.* **256**, 187 (1996).
- 58 D. A. Debe and W. A. Goddard III, *J. Mol. Biol.* **294**, 619 (1999).
- 59 G. A. Mines, T. Pascher, S. C. Lee, J. R. Winkler, and H. B. Gray, *Chem. Biol.* **3**, 491 (1996).
- 60 C. Chan, Y. Hu, S. Takahashi, D. L. Rousseau, W. A. Eaton, and J. Hofrichter, *Proc. Natl. Acad. Sci. USA* **94**, 1779 (1997).
- 61 C. K. Smith, Z. M. Bu, J. M. S. K. S. Anderson, D. M. Engelman, and L. Regan, *Protein Sci* **5**, 2009 (1996).
- 62 M. L. Scalley, Q. Yi, H. D. Gu, A. McCormack, J. R. Yates, and D. Baker, *Biochemistry* **36**, 3373 (1997).
- 63 S. E. Jackson and A. R. Fersht, *Biochemistry* **30**, 10428 (1991).
- 64 Y.-J. Tan, M. Oliveberg, and A. R. Fersht, *J. Mol. Biol.* **264**, 377 (1996).
- 65 N. A. J. Van Nuland, W. Meijberg, J. Warner, V. Forge, R. M. Schee, G. T. Robillard, and C. M. Dobson, *Biochemistry* **37**, 622 (1998).
- 66 V. Villegas, A. Azuaga, L. Catasus, D. Reverter, P. L. Mateo, F. X. Aviles, and L. Serrano, *Biochemistry* **34**, 15105 (1995).
- 67 M. Silow and M. Oliveberg, *Biochemistry* **36**, 7633 (1997).
- 68 N. Taddei, F. Chiti, P. Paoli, T. Fiaschi, M. Bucciattini, M. Stefani, C. M. Dobson, and G. Ramponi, *Biochemistry* **38**, 2135 (1999).
- 69 S. E. Jackson, *Folding and Design* **3**, R81 (1998).
- 70 V. P. Grantcharova and D. Baker, *Biochemistry* **36**, 15685 (1997).
- 71 K. Plaxco, J. Guijarro, C. Morton, M. Pitkeathly, I. Campbell, and C. Dobson, *Biochemistry* **37**, 2529 (1998).
- 72 D. Perl, C. Welker, T. Schindler, K. Schroeder, M. A. Marahiel, R. Jaenicke, and F. Schmid, *Nat. Struct. Biol.* **5**, 229 (1998).
- 73 K. L. Reid, H. M. Rodriguez, B. J. Hillier, and L. M. Gregoret, *Protein Sci.* **7**, 470 (1998).
- 74 N. Schonbrunner, K. P. Kofler, and T. Kiefhaber, *J. Mol. Biol.* **268**, 526 (1997).
- 75 I. Guijarro, C. Morton, K. W. Plaxco, I. D. Campbell, and C. Dobson, *J. Mol. Biol.* **276**, 657 (1998).
- 76 J. Clarke, S. J. Hamill, and C. M. Johnson, *J. Mol. Biol.* **270**, 771 (1997).
- 77 J. Clarke, E. Cota, S. B. Fowler, and S. J. Hamill, *Structure* **7**, 1145 (1999).

Protein	Length	Family	$\ln K_f$
1shg ⁵³	57	α	2.10
1lmb ^{54,55}	80	α	8.50
2abd ^{56,57}	86	α	6.55
1imq ⁵⁸	86	α	7.31
1ycc ⁵⁹	103	α	9.61
1hrc ⁶⁰	104	α	7.94
1hrc, horse, oxidized Fe ^{III} ⁶⁰	104	α	5.99
2gb1 ⁶¹	56	α/β	6.26
2pt1 ⁶²	61	α/β	4.22
2ci2 ⁶³	65	α/β	3.87
1cis ⁶⁴	66	α/β	3.87
1hdn ⁶⁵	85	α/β	2.70
1aye ⁶⁶	92	α/β	6.80
1urn ⁶⁷	96	α/β	5.73
1aps ⁶⁸	98	α/β	-1.47
1fkb ⁶⁹	107	α/β	1.46
2vik ⁶⁹	126	α/β	6.80
1srl ⁷⁰	56	β	4.04
1shf.a ⁷¹	59	β	4.55
1tud ⁵⁸	60	β	3.45
1csp ⁷²	67	β	6.04
1mjc ⁷³	69	β	5.23
3mef ⁷³	69	β	5.30
2ait ⁷⁴	74	β	4.20
1pks ⁷⁵	76	β	-1.05
1ten ⁷⁶	89	β	-1.10
1fmf, 9FN-III ⁷⁷	90	β	-0.90
1wit ⁷⁷	93	β	0.41
1fmf, 10FN-III ⁷⁷	94	β	5.00

TABLE I: List of proteins known to fold via a two-state mechanism. The experimental quantities K_F (s^{-1}) are desumed from the cited references.

Protein (X-ray)	Length	B-factor corr.	Protein (NMR)	Length	B-factor corr.
1AIL	70	0.754	1A1W	82	0.878
1AMM	174	0.722	1A23	188	0.806
1BEO	98	0.541	1AA9	170	0.745
1BFG	126	0.544	1AQR	39	0.874
1CEI	85	0.734	1BO0	75	0.969
1CEX	197	0.723	1FLS	156	0.592
1CHD	198	0.774	1GHT	104	0.955
1COF	135	0.657	1JLI	111	0.891
1FNA	91	0.390	1OCD	103	0.532
1FXD	58	0.572	1TRS	104	0.549
1GPR	158	0.616	1A8C	80	0.355
1HOE	74	0.636	1AHK	128	0.678
1IDO	184	0.378	1AWJ	76	0.371
1IGD	61	0.444	1BUY	165	0.726
1KID	193	0.662	1FWQ	114	0.910
1KUH	132	0.545	1IKL	68	0.962
1LAA	130	0.552	1JOO	148	0.903
1LCL	141	0.754	1TAM	119	0.703
1MAI	119	0.722	1AA3	62	0.809
1NPK	150	0.524	1AK6	173	0.929
1OPD	85	0.446	1BHU	101	0.348
1PDR	96	0.596	1EZA	258	0.842
1PKP	145	0.771	1GDF	144	0.980
1POA	118	0.658	1IL6	165	0.587
1SFE	165	0.633	1LXL	220	0.895
1SHG	57	0.580	1TBD	133	0.853
1THV	207	0.771			
1VCC	77	0.690			
1VHH	157	0.741			
1VSD	146	0.557			

TABLE II: List of single-chain X-ray and NMR proteins representative of distinct structural classes. The linear correlation coefficient between the experimental values for the B-factors and the theoretical ones (calculated at $T = 0$ are quoted for each entry).